

A theoretical study of Gemini surfactant phase behavior

Kristine M. Layn, Pablo G. Debenedetti, and Robert K. Prud'homme^{a)}

Department of Chemical Engineering, Princeton University, Princeton, New Jersey 08544

(Received 14 November 1997; accepted 8 April 1998)

Gemini surfactants are a relatively new type of surface active material, characterized by multiple hydrophilic head groups. The phase behavior of a Gemini surfactant lattice model is studied by Monte Carlo simulations and quasicheical (QC) calculations. The predictions of these methods are in excellent agreement, justifying use of the analytical QC theory. The dependence on temperature, surfactant solubility, surfactant rigidity, and oil chain length of the global phase behavior of ternary mixtures of Gemini surfactant, oil, and water is investigated. Three-phase equilibrium exists only at low temperatures, with a transition to two-phase equilibrium as temperature is increased. Surfactants with moderate solubilities (i.e., those which do not have a strong preference for either solvent) exhibit three-phase equilibrium at low temperatures, while surfactants with extreme solubility preferences yield two-phase equilibrium only. When a flexible surfactant exhibits three-phase equilibrium, imposing rigidity promotes a transition from three- to two-phase equilibrium. Increasing molecular size of the hydrophobic solvent (oil) causes a transition from two- to three-phase equilibrium, and finally back to two-phase equilibrium, but with reversed relative surfactant solubility in the oil and water phases. © 1998 American Institute of Physics. [S0021-9606(98)51127-0]

I. INTRODUCTION

While conventional, or simple, surfactants consist of a single hydrophilic head and one or two hydrophobic tails, Gemini surfactants are characterized by multiple head groups. The name Gemini was first applied to surfactants in 1991, at which time it referred exclusively to two identical simple surfactants joined by a spacer between the heads.¹ Since then, the label Gemini has broadened to encompass any surfactant having two or more head groups and any number of tails. Several Gemini surfactants are shown in Fig. 1.

Experimental studies of Gemini surfactants have revealed intriguing behavior of significant practical interest. Critical micelle concentration (CMC) and C_{20} (surfactant concentration required to reduce surface tension by 20 dyn/cm) values for Geminis are generally much lower than those of the corresponding monomers. Typical behavior is illustrated in Table I, which shows differences of several orders of magnitude between CMC and C_{20} data for selected Geminis and their analogous simple surfactants.⁵ CMC and C_{20} values are indicators of surface activity, with smaller values corresponding to greater surface activity and a more efficient surfactant. Another property for which Geminis differ from simple surfactants is aggregation morphology. As one example, aqueous solutions of the Gemini shown in Fig. 1(c) assemble into highly branched, threadlike micelles, while the corresponding monomer forms only spherical micelles.⁶ In addition to high surface activity and branched microstructures, Geminis exhibit such interesting phenomena as anomalous CMC dependence on hydrophobicity and signifi-

cant hydrophobe solvation at the air-water interface.¹

The number of potential Gemini structures is enormous. In addition to structural variables associated with simple surfactants (such as tail length and degree of branching, ionic nature of the head group, and counterion type), Geminis are also characterized by the number of heads (dimer, trimer, tetramer, etc.), spacer solubility (i.e., hydrophilic or hydrophobic), spacer length, and molecular rigidity. This last property is determined largely by spacer type. Flexible spacers (such as methylene chains) allow the head groups to move relative to one another, and to adopt a preferred separation distance and orientation based on solvation energetics and entropic considerations. Inflexible spacers (such as stilbene derivatives¹) restrict the relative positions of the head groups and result in rigid molecules.

The novel properties associated with Gemini surfactants have motivated efforts to synthesize new Gemini structures with the hope that they will possess desirable characteristics. While the large number of Gemini structural variables makes such a trial and error approach inefficient, efforts to make judicious choice of the surfactant structure prior to synthesis are hindered by a lack of fundamental understanding of the qualitative relationships between molecular structure and macroscopic properties. Our goal is to develop these relationships, via theoretical and computational methods, in an attempt to guide future synthetic efforts.

The focus of the present work is the phase behavior of Gemini surfactant systems. Section II describes the model and two methods (one computational and one theoretical) used to calculate phase diagrams. A comparison of results from these methods shows excellent agreement and justifies use of the analytical theory. Section III summarizes the key results of a detailed theoretical study of phase behavior, including the effect of temperature, surfactant solubility, sur-

^{a)}Author to whom correspondence should be addressed; Phone (609) 258-4577; Fax (609) 258-0211; Electronic mail: prudhomm@princeton.edu.

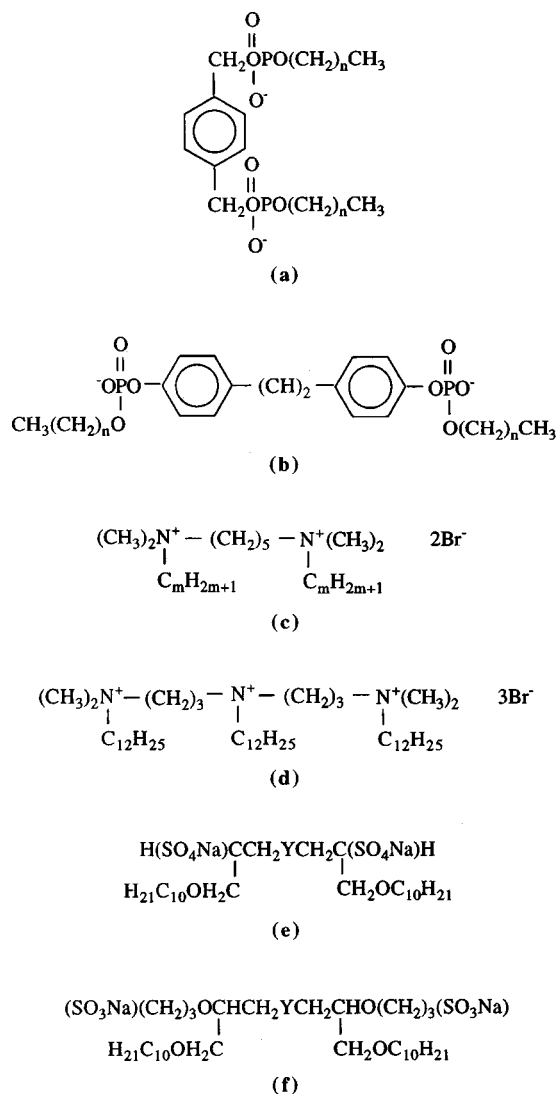


FIG. 1. Representative Gemini surfactants. (a) Xylylene diphosphate (Ref. 1); (b) Diphosphate with rigid stilbene spacer (Ref. 2); (c) Bis(dimethylalkylammonium bromide) dimer (Ref. 3); (d) Trimeric analog of (c) (Ref. 4) (e),(f) Disulfate (Ref. 5); Y = $\text{OCH}_2\text{CH}_2\text{O}$, O , $\text{OCH}_2\text{CH}_2\text{O}$, $\text{O}(\text{CH}_2\text{CH}_2\text{O})_2$.

factant rigidity, and oil chain length. Section IV concludes with a summary and Sec. V identifies relevant questions currently under investigation.

II. MODEL AND METHODS

A. The model

The goal of this study is to investigate general trends in global phase behavior; the model therefore incorporates only

TABLE I. CMC and C_{20} data for several Gemini surfactants and their monomeric (simple surfactant) analogs (Ref. 2).

		Y	CMC (mM)	C_{20} (mM)
Gemini monomer	Figure 1(e)	$-\text{OCH}_2\text{CH}_2\text{O}-$	0.013	0.0010
	$\text{C}_{12}\text{H}_{25}\text{SO}_4\text{Na}$...	8.2	3.1
Gemini monomer	Figure 1(f)	$-\text{O}-$	0.033	0.008
Gemini monomer	Figure 1(f)	$-\text{OCH}_2\text{CH}_2\text{O}-$	0.032	0.0065
Gemini monomer	Figure 1(f)	$-\text{O}(\text{CH}_2\text{CH}_2\text{O})_2-$	0.060	0.0010
	$\text{C}_{12}\text{H}_{25}\text{SO}_3\text{Na}$...	9.8	4.4

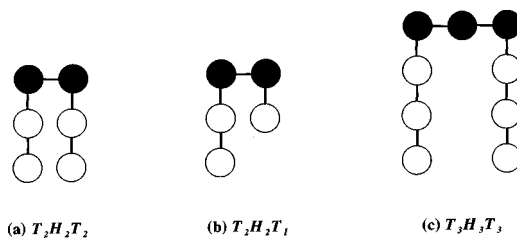


FIG. 2. Model Gemini surfactants. Open circles represent hydrophobic tail segments and filled circles represent hydrophilic segments (head or spacer).

the most essential features of Gemini surfactant mixtures. The system consists of a simple cubic lattice fully occupied by surfactant, water, and oil molecules. A surfactant is represented by a connected string of head and tail units, each of which occupies a single lattice site. Figure 2 shows typical model structures. Surfactants are labeled $T_iH_jT_k$ where i and k refer to tail lengths and j is the combined number of head and hydrophilic spacer units.

A surfactant head unit is energetically equivalent to water and a tail unit is energetically equivalent to oil. Thus a surfactant is represented by a string of ‘‘waterlike’’ and ‘‘oil-like’’ particles, and each site may be energetically characterized as hydrophilic or hydrophobic. These interactions are expected to capture the basic features of a surfactant system, but are unrealistic in several important ways. No driving force is imposed to favor the preferential solvation of head units with water as opposed to other heads, or of tail units with oil rather than other tails. This allows surfactants to reduce unfavorable contacts by self-aggregating rather than partitioning to oil–water interfaces.⁷ In addition, attractive head interactions neglect the electrostatic repulsion associated with ionic head groups. Despite such simplifications, these interaction energies have proven successful in the study of monomeric surfactants.^{7–9}

B. Computational method

Previous efforts to predict the phase behavior of simple surfactant systems have involved two computational methods. Early work by Larson and co-workers estimated free energy through numerical integration of the Gibbs–Helmholtz equation using average energies obtained from canonical ensemble Monte Carlo simulations.^{7,8} Although this approach is thermodynamically rigorous, it suffers from an inability to distinguish two- and three-phase equilibrium and is computationally expensive as a series of simulations is required to generate a single tie line. Most importantly, it requires that the model surfactant be symmetric, which precludes application of the method to Gemini surfactants. More recently, Panagiotopoulos and co-workers have utilized Gibbs ensemble simulations.⁹ While this method is very convenient for the investigation of systems of small molecules which do not have a tendency to form ordered structures, the connected nature of microemulsions reduces its efficiency and raises concerns regarding adequate sampling of low energy states.

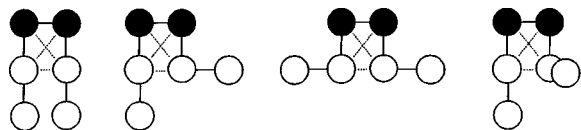
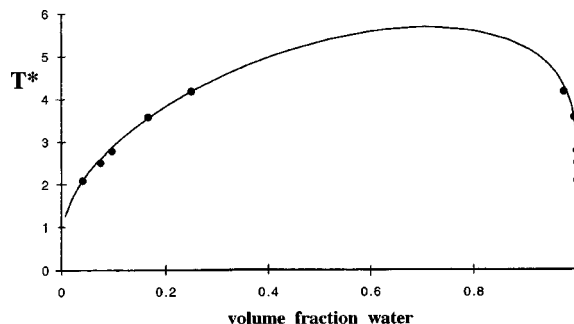


FIG. 3. Configurations of $T_2H_2T_2$ that are allowed by an imposed rigidity constraint. When this molecule is treated as rigid, the intramolecular contacts marked by dashed lines are not available for solvation and are not included in the counting of contacts in the QC treatment.

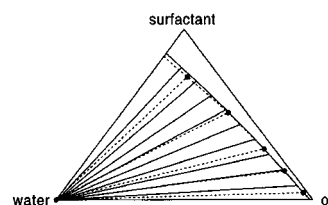
These considerations motivated the use of a different computational method in this work, namely block composition distributions.^{10,11} Following equilibration of a canonical ensemble Monte Carlo simulation, the composition of a small subcell placed at a random position in the simulation box is sampled over a large number of configurations. For a ternary system (oil, water, and surfactant), the probability distribution of subcell composition is a three-dimensional surface. When the bulk (overall system) composition is in a single-phase region, this surface exhibits a single peak at the bulk composition. When the bulk composition is in a phase-separated region, local composition fluctuations reflect equilibrium phase compositions, resulting in a multimodal frequency surface with each peak centered at the composition of an equilibrium phase. With this method, a single canonical ensemble simulation may yield the endpoints of a tie line. In practice, several simulations are sometimes necessary as the bulk composition must be chosen such that multiple peaks are of roughly the same height. If the bulk composition is too close to the composition of one of the equilibrium phases, the peak for this phase will dominate the frequency surface and may alter the positions of other peaks, or in extreme cases, render a second peak undetectable.

One of the most significant limitations of this method is an inability to provide a precise estimate of the critical point. As the bulk composition moves closer to the critical point, equilibrium phases approach the same composition. Because peaks in the frequency surface are centered at the equilibrium phase compositions, peaks begin to overlap before the critical point is reached. Although estimates of the critical point may be extracted from finite-size scaling techniques, such an approach requires long simulations of large systems and is computationally expensive even for simple, single component systems.^{12,13}

Simulations are performed on an n^3 simple cubic lattice, with a cubic subcell of size b^3 . The efficiency of surfactant moves is improved by a standard Rosenbluth configurational bias scheme.¹⁴ The optimal ratio of subcell to overall system size is dependent on surfactant length and is determined by trial and error. If the subcell is too large, phase separation will occur within the cell. While a small subcell avoids this and reduces computation time, the subcell size is limited from below by composition resolution (the smaller the subcell the fewer compositions which may be observed) and by peak resolution (when the subcell is too small, multiple peaks overlap). The majority of simulations were performed for a $T_2H_2T_2$ surfactant, for which 15 and five were found to be adequate values of n and b , respectively.



(a)



(b)

FIG. 4. Comparison of QC and simulation results. (a) $T_2H_2T_2$ and water; $z = 26$; $T^* = kT/\epsilon$; solid line, QC, circles, simulation ($n = 15$, $b = 5$). (b) $T_2H_2T_2$, water, and oil; $z = 6$; $T^* = 1.33$; solid lines, QC, dashed lines and circles, simulation ($n = 15$, $b = 5$).

C. Theoretical method

The quasichemical (QC) theory of Guggenheim¹⁵ was investigated as a simple, analytical alternative to the computational block distribution method. The QC theory assumes independence of contact pairs and maximizes the resulting configurational partition function to yield the following relation between the number of ij contacts, X_{ij} :

$$\frac{X_{ij}^2}{X_{ii}X_{jj}} = 4e^{-2\epsilon_{ij}/kT}, \quad (1)$$

where ϵ_{ij} is the exchange energy of an ij pair [i.e., $\epsilon_{ij} = E_{ij} - 0.5(E_{ii} + E_{jj})$, where E_{ij} is the interaction energy of an ij pair].

The free energy of mixing obtained by integrating the Gibbs–Helmholtz equation is differentiated with respect to mole number to yield the following expression for the change in chemical potential of species i upon mixing:

$$\frac{\Delta\mu_i}{kT} = \ln \vartheta_i + \frac{1}{2}zq_i \ln \frac{\xi_i}{\vartheta_i} + \frac{1}{2}zq_i h_i \ln \frac{h_i(1-\kappa t)}{h(1-\kappa_i t_i)} + \frac{1}{2}zq_i t_i \ln \frac{t_i(1-\kappa h)}{t(1-\kappa_i h_i)}, \quad (2)$$

where z is the coordination number, zq_i is the number of contacts for each molecule of species i , h_i is the fraction of species i contacts which are hydrophilic, $t_i = 1 - h_i$, ϑ_i is the volume fraction of species i , ξ_i is the fraction of all contacts which originate from i molecules, $h = \sum \xi_i h_i$, and $t = \sum \xi_i t_i$. κ is the root of $1 - \kappa = \kappa^2 h t (e^{2\epsilon/kT} - 1)$ which lies between zero and two and κ_i is the same quantity for pure component

TABLE II. Summary of systems studied.

	r_s	h_s	zq_s	T^* range	Three-phase equilibrium
$T_1H_2T_1$	4	0.49	98	3.8 – 10.0	x
$T_2H_2T_1$	5	0.39	122	3.3 – 10.0	x
$T_1H_3T_1$	5	0.59	122	3.8 – 10.0	
$T_2H_2T_2$	6	0.33	146	3.3 – 11.1	
$T_2H_3T_1$	6	0.49	146	3.3 – 10.0	x
$T_1H_4T_1$	6	0.66	146	2.9 – 10.0	
$T_2H_3T_2$	7	0.42	170	4.0 – 10.0	x
$T_2H_4T_2$	8	0.49	194	4.0 – 10.0	x
$T_3H_3T_3$	9	0.33	218	2.9 – 10.0	
$T_3H_4T_2$	9	0.44	218	4.0 – 10.0	x
$T_2H_5T_2$	9	0.55	218	4.0 – 10.0	x
$T_2H_6T_1$	9	0.66	218	4.0 – 10.0	
$T_1H_7T_1$	9	0.77	218	4.0 – 10.0	
$T_3H_4T_3$	10	0.40	242	4.0 – 10.0	x
$T_4H_4T_3$	11	0.36	266	4.0 – 10.0	
$T_3H_5T_3$	11	0.45	266	4.0 – 10.0	x
$T_3H_6T_2$	11	0.54	266	4.0 – 10.0	x
$T_2H_7T_2$	11	0.63	266	4.0 – 10.0	
$T_2H_8T_1$	11	0.72	266	4.0 – 10.0	
$T_1H_9T_1$	11	0.81	266	4.0 – 10.0	
$T_6H_4T_5$	15	0.27	362	4.0 – 10.0	
$T_5H_5T_5$	15	0.33	362	4.0 – 11.0	
$T_5H_6T_4$	15	0.40	362	4.0 – 10.0	
$T_4H_7T_4$	15	0.46	362	4.0 – 10.0	x
$T_4H_8T_3$	15	0.53	362	4.0 – 10.0	x
$T_3H_9T_3$	15	0.60	362	4.0 – 10.0	x
$T_3H_{10}T_2$	15	0.66	362	4.0 – 10.0	

i . κ_i is obtained by replacing h by h_i , t by t_i , and ϵ (the exchange energy of a hydrophilic–hydrophobic pair) by zero if species i has only one type of contact (i.e., is oil or water).¹⁶ The molecular structure variables which must be specified are zq_i , h_i , and r_i , the number of sites occupied by each molecule of species i .

When a single system exhibits multiple phase envelopes, the nature of overlap between the envelopes determines whether the system is in two- or three-phase equilibrium. Partial overlap of phase envelopes is characteristic of three-phase equilibrium. Because the composition at which overlap first occurs is the endpoint of a tieline in each envelope, this composition is in equilibrium with two other compositions, and therefore all three compositions are in equilibrium. When multiple phase envelopes overlap such that one envelope is completely within the other, one envelope is metastable. The stable envelope is identified by choosing a bulk composition in the overlap region and comparing the free energy of the system assuming separation along one set of tie lines to the free energy assuming separation along the other set of tie lines. The stable phase envelope yields a lower free energy.

As mentioned previously, Gemini surfactants range from very flexible to very rigid, depending on the nature of the spacer. In the limit of a completely flexible spacer, there are no intrinsic barriers to configurational changes; the surfactant is free to adopt any configuration, and the most favorable one

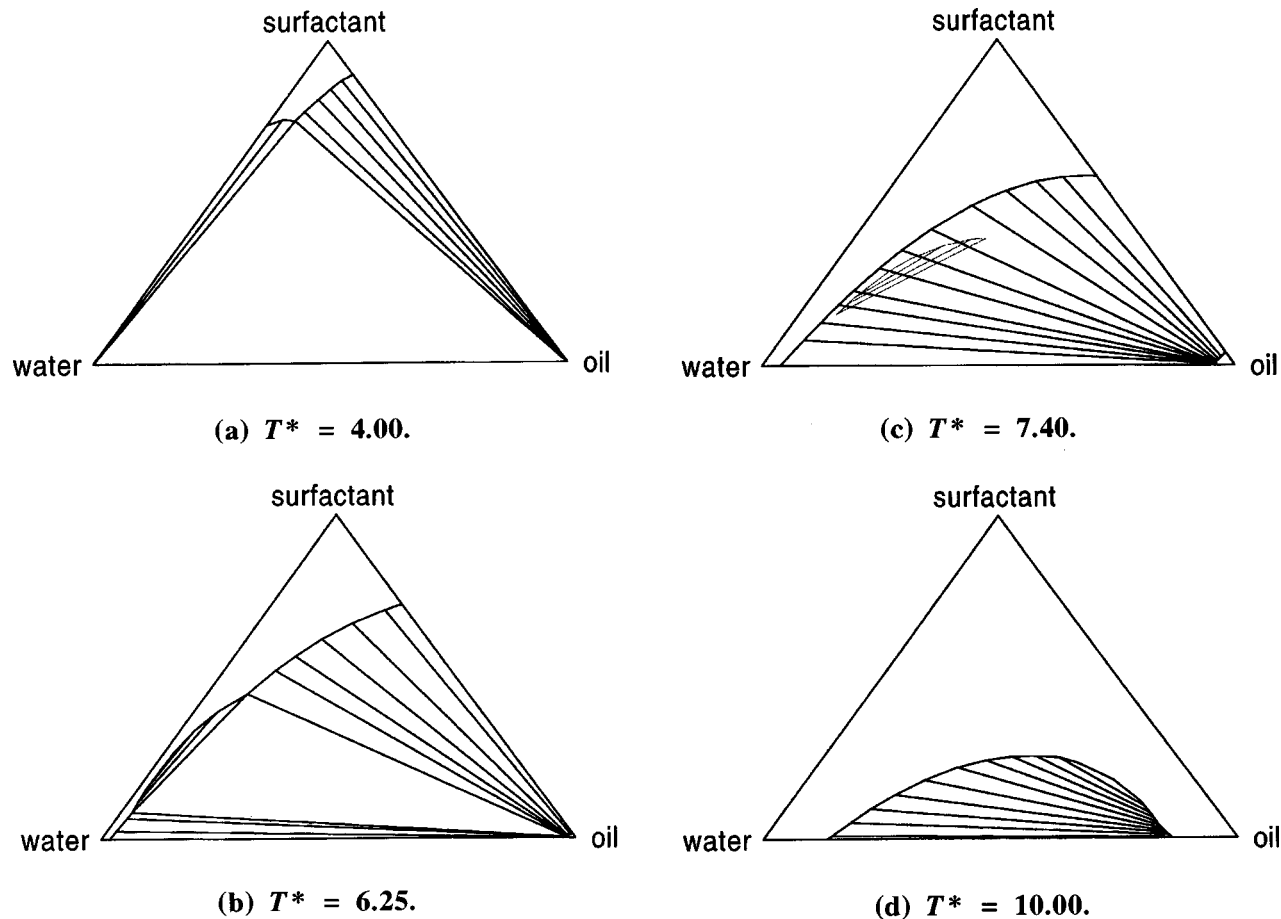


FIG. 5. The effect of temperature on the phase behavior of $T_2H_5T_2$; $r_s=9$, $zq_s=218$, $h_s=0.55$.

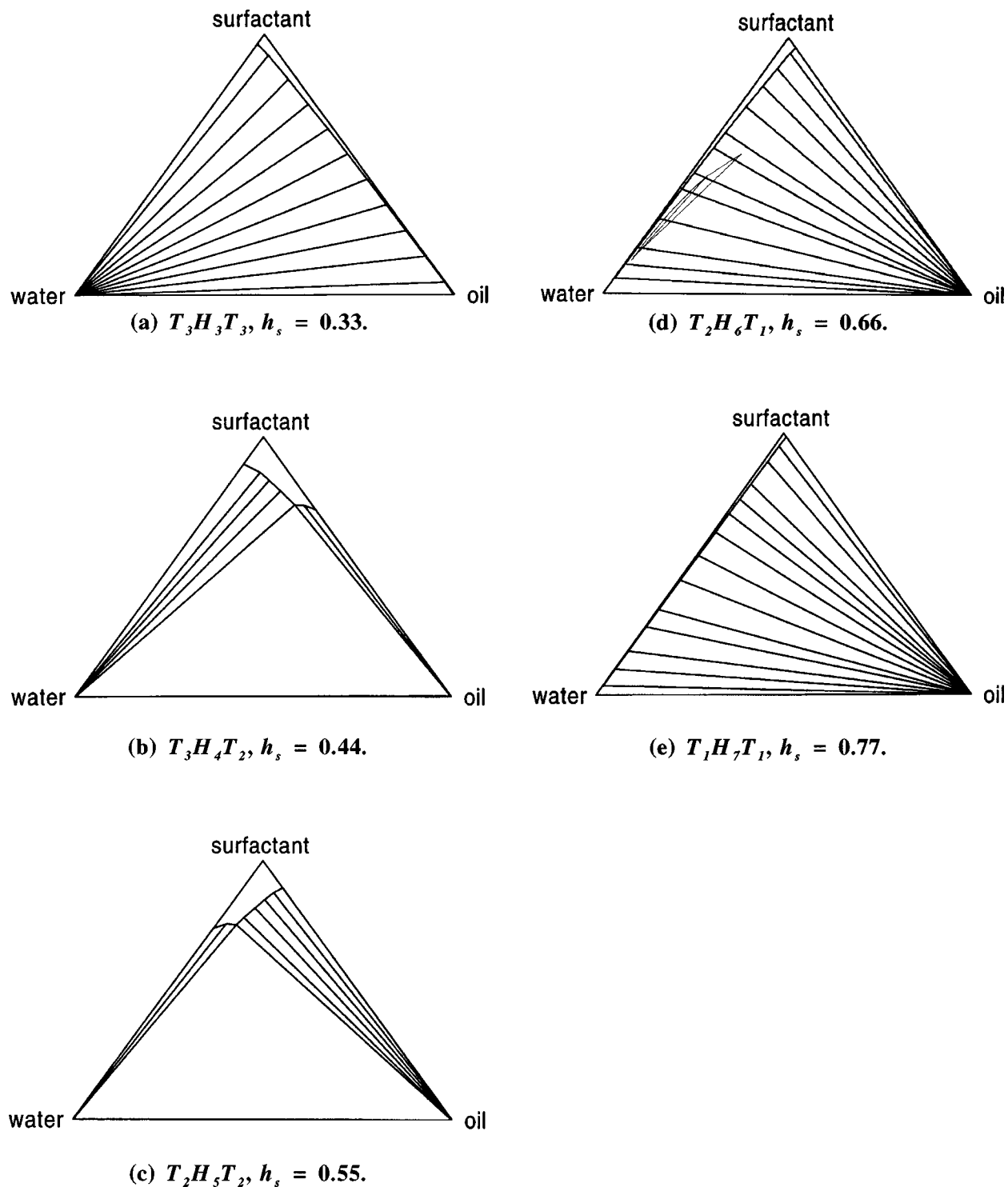


FIG. 6. The effect of surfactant solubility on the phase behavior of Geminis occupying nine sites; $r_s=9$, $zq_s=218$, $T^*=4.0$.

will be determined by solvation effects. In the opposite extreme of a completely rigid spacer, intramolecular motion is restricted and the configuration of the surfactant is dictated by rigid bonds rather than neighboring solvent contacts.

For simplicity, we limit this study to the cases of completely flexible or completely rigid surfactants. As molecular rigidity originates from bonds in the spacer, we choose to define configurations by the relative positions of all head and spacer units and the tail units directly bonded to the heads.

The positions of the remaining tail segments are not restricted as they represent flexible long chain hydrocarbons.

Because a flexible molecule may adopt any configuration, all of the contacts along the chain are available for solvation. In contrast, a completely rigid molecule exists in a single configuration exclusively, and this may prevent some contacts along the chain from interacting with solvent molecules. Figure 3 shows several configurations of $T_2H_2T_2$ that are allowed by a particular rigidity constraint. When this

molecule is treated as rigid, the contacts marked by dashed lines are no longer available for solvation. In the context of the QC theory, the rigidity constraint is introduced simply by excluding these fixed intramolecular contacts from the total number of contacts. This simple result is due to the calculation of equilibrium phase compositions via free energies of mixing; the fixed intramolecular contacts resulting from molecular rigidity are equivalent in both pure and mixed states, and hence make no contribution to mixing energies.

Although this treatment of surfactant rigidity is theoretically rigorous within the framework of the QC theory, it is simplistic in regard to surfactant connectivity. Because the QC theory accounts only for contact pairs, the structure of the chain molecule is considered only in the counting of pair interactions. Thus the actual configuration adopted by the surfactant is reflected only through the intramolecular contacts which become fixed and consequently unavailable for solvation. The relative positions of the remaining contacts are neglected, as are any entropic effects which may result from constraining the chain configuration.

D. Method comparison

A comparison of phase diagrams from QC theory calculations and block composition distributions shows excellent agreement between the two methods. A comparison was made for binary (surfactant and water) and ternary (surfactant, water, and oil) systems, for several surfactant structures, over a range of temperatures, and for coordination numbers of six (nearest-neighbor interactions only) and 26 (nearest- and diagonal nearest-neighbor interactions). Figure 4 shows essentially exact quantitative agreement between the predictions of both methods for binary and ternary systems of the Gemini $T_2H_2T_2$. At least qualitative agreement was found in all cases considered, suggesting that the analytical QC theory captures the essential features of the problem. This very satisfactory agreement between theory and simulations is not expected to hold for longer molecules and lower temperatures, where a significant amount of molecular association will occur. The quasicheical theory, which takes into account nearest-neighbor interactions only, is incapable of capturing long-range association.

In light of the agreement between the quasicheical theory and the Monte Carlo simulations and the significant CPU demands of the computational approach, the detailed study discussed in the following section was performed with the quasicheical theory theory.

III. RESULTS

Results are presented to illustrate the effect of temperature, surfactant solubility, surfactant rigidity, and oil chain length on phase separation. Table II summarizes the systems and conditions studied; results discussed below are representative of the behavior observed for all systems considered. All calculations are performed with a coordination number of 26. Water is a single site species. Unless otherwise stated, the oil molecule is a single site species and surfactants are completely flexible (all contacts along the chain are counted).

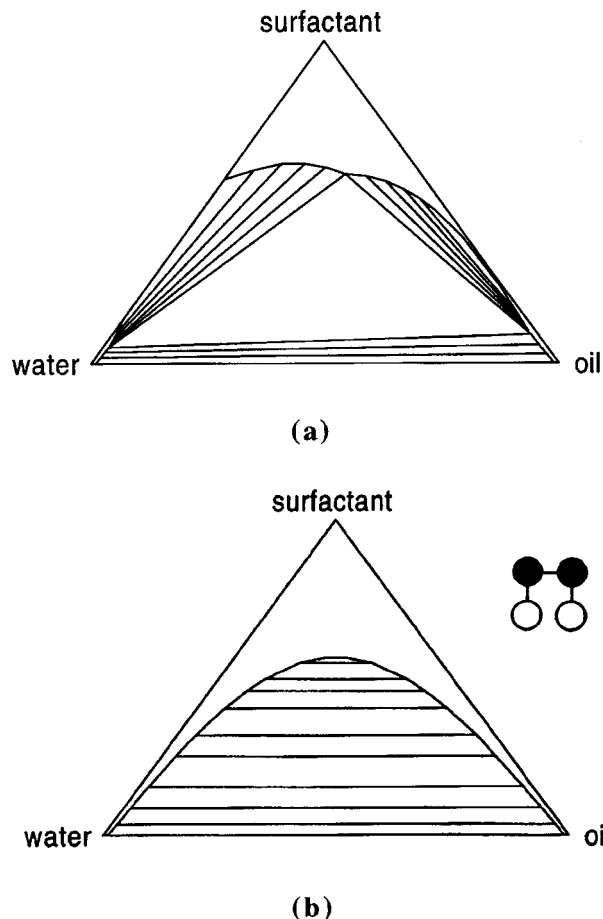


FIG. 7. The effect of surfactant rigidity on the phase behavior of $T_1H_2T_1$; $T^*=5.55$, $r_s=4$. (a) Flexible $T_1H_2T_1$; $z_{q_s}=98$, $h_s=0.49$. (b) Rigid $T_1H_2T_1$; $z_{q_s}=92$, $h_s=0.50$.

A. Temperature

Figure 5 illustrates the phase behavior of $T_2H_5T_2$ over a series of dimensionless temperatures ($T^*=kT/\epsilon$). At low temperatures [Fig. 5(a)], the system exhibits a three-phase triangle surrounded on two sides by two-phase envelopes. There is a miscibility gap along both the oil-surfactant and water-surfactant axis. An increase in temperature [Fig. 5(b)] yields a third two-phase region below the three-phase triangle, decreases the size of the three-phase region, and eliminates the surfactant-water miscibility gap. At higher temperatures, the three-phase triangle is replaced by a stable two-phase region [Fig. 5(c), large envelope] and a metastable region [Fig. 5(c), small envelope]. At high temperatures [Fig. 5(d)] both the metastable region and the surfactant-oil immiscibility are eliminated.

B. Surfactant solubility

The effect of surfactant solubility is illustrated by Fig. 6. All of the surfactant structures depicted occupy nine sites ($r_s=9$) and have the same number of contacts ($z_{q_s}=218$). The only remaining variable is h_s , the fraction of surfactant contacts that are hydrophilic. Physically, h_s is representative of the molecule's hydrophilic-lyophilic balance

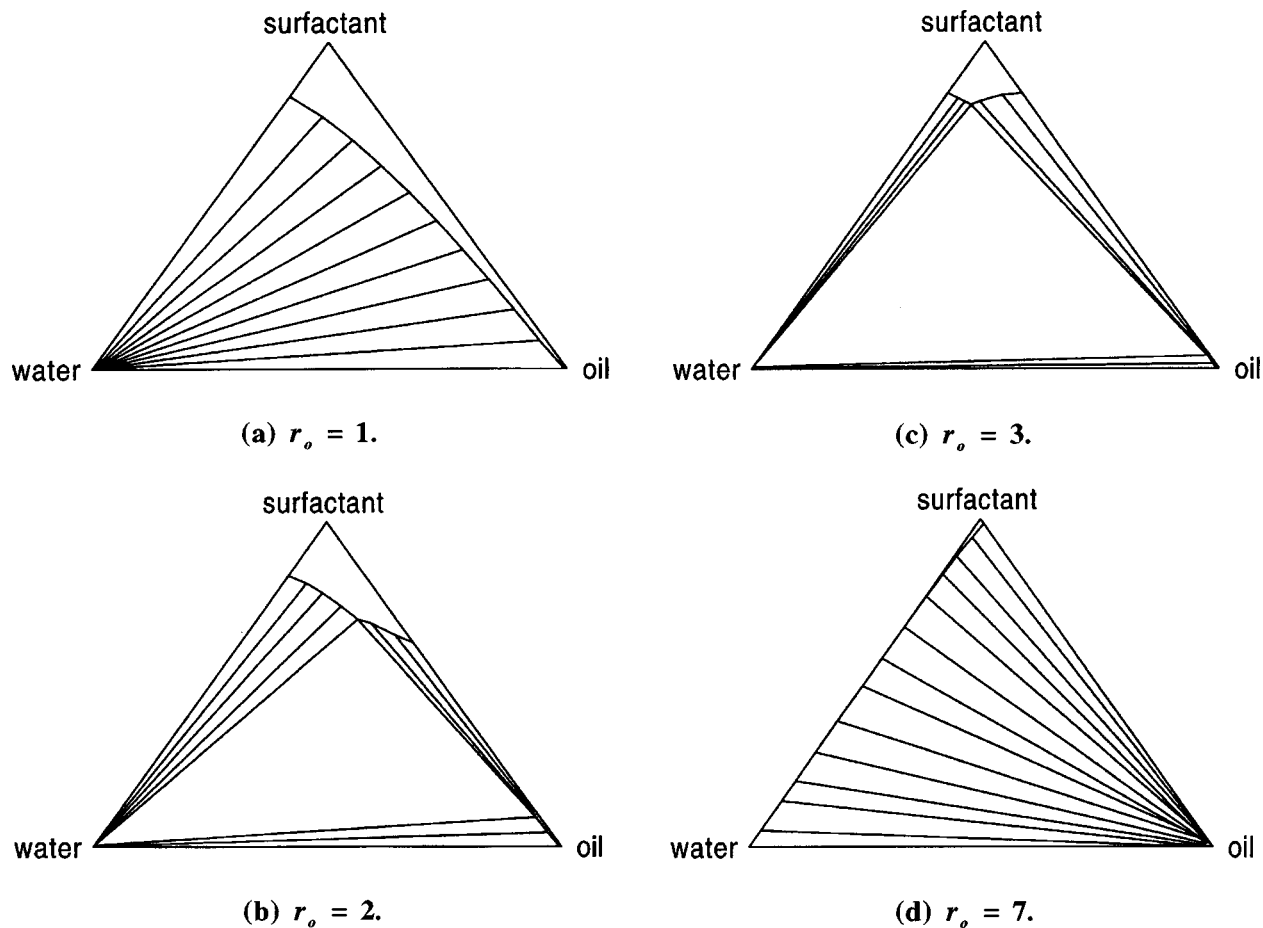


FIG. 8. The effect of oil chain length on the phase behavior of $T_2H_2T_1$; $r_s=5$, $h_s=0.39$, $T^*=5.56$; r_o is the number of sites occupied by an oil molecule.

(HLB); the surfactant becomes more hydrophobic as h_s is decreased below 0.5 and more hydrophilic as h_s is increased above 0.5.

The progression from Fig. 6(a) to Fig. 6(e) is an increase in the ratio of hydrophilic to hydrophobic units. The most hydrophobic surfactant [Fig. 6(a)] exhibits only two-phase equilibrium, with the surfactant more soluble in the oil-rich phase. Increasing h_s by replacing a tail segment by a hydrophilic spacer unit results in a three-phase triangle surrounded by two-phase envelopes [Fig. 6(b)]. The larger two-phase region is the one for which the surfactant is more soluble in the oil-rich phase, as expected due to the hydrophobic character of the surfactant ($h_s < 0.5$). Increasing h_s to 0.55 yields a slightly hydrophilic surfactant which again exhibits a three-phase triangle [Fig. 6(c)]. The dominant two-phase region is now the one for which the surfactant is more soluble in the water-rich phase. An increase in h_s to 0.66 [Fig. 6(d)] causes a transition to two-phase equilibrium with a small metastable region near the edge of the stable envelope. The metastable region is eliminated by a further increase in h_s [Fig. 6(e)].

The combined behavior of all systems studied suggests that three-phase equilibrium will exist at low temperatures if the surfactant is only moderately hydrophilic or hydrophobic. Extreme surfactant solubility preferences yield two-phase equilibrium, with an essentially pure oil or water phase in equilibrium with surfactant and the remaining solvent. The physical cause of this behavior is clear; three-phase equilib-

rium is the result of partial overlap of two separate phase envelopes, one for which the surfactant is more soluble in the water-rich phase and one for which the surfactant is more soluble in the oil-rich phase. Such behavior will occur if the surfactant has only a weak preference for one solvent.

C. Surfactant rigidity

As discussed previously, imposing rigidity on a chain molecule fixes intramolecular contacts and thereby reduces the number of contacts available for solvation. In the context of the QC theory, this results in a decrease in zq_s , the number of surfactant contacts. In general, this may be accompanied by a change in h_s , the fraction of surfactant contacts which are hydrophilic.

The effect of imposing rigidity is illustrated by Fig. 7. Figure 7(a) corresponds to a completely flexible $T_1H_2T_1$ ($zq_s=98$, $h_s=0.49$) and Fig. 7(b) to a completely rigid $T_1H_2T_1$ which is constrained to lie in the configuration depicted ($zq_s=92$, $h_s=0.50$). The flexible molecule exhibits a three-phase region which is lost when rigidity is imposed. Although h_s for the rigid case is slightly larger, the difference is small compared to the difference in the number of contacts. The surfactant solubility study discussed above suggests that such a small difference in h_s is not likely to have a significant impact on phase behavior; the expected

cause of the transition from three- to two-phase equilibrium is loss of contacts.

Phase diagrams of rigid surfactants were calculated for all possible configurations of $T_1H_2T_1$ and $T_2H_2T_1$. With the exception of one configuration of $T_1H_2T_1$, all rigid configurations studied showed similar behavior (loss of the three-phase region exhibited by the flexible molecule); the exception was for the case of the smallest decrease in the number of contacts ($zq_s=98$ for the flexible molecule and 96 for the rigid).

D. Hydrophobic solvent chain length

Figure 8 shows the effect of the hydrophobic solvent (oil) chain length on the phase behavior of the Gemini $T_2H_2T_1$. A single site oil molecule [Fig. 8(a)] results in two-phase equilibrium with the surfactant partitioning to the oil-rich phase. Increasing the oil length to two [Fig. 8(b)] results in a three-phase triangle with the larger two-phase region corresponding to the surfactant existing preferentially in the oil-rich phase. The three-phase region is retained for an oil length of three [Fig. 8(c)], but the dominant two-phase envelope corresponds to the surfactant being more soluble in the water-rich phase. For sufficiently long oil molecules [Fig. 8(d)], the system reverts to two-phase equilibrium with reversed surfactant solubility (surfactant is more soluble in the aqueous phase).

IV. SUMMARY

The phase behavior of Gemini surfactant systems has been investigated by computational and theoretical methods. The predictions of both methods are generally in quantitative agreement, justifying extensive use of the simpler theoretical approach. A detailed study of relevant system variables has led to general conclusions regarding the effect of temperature, surfactant solubility, surfactant rigidity, and oil chain length on phase behavior.

Gemini surfactants which are moderately hydrophilic or hydrophobic ($0.39 \leq h_s \leq 0.60$ for the systems studied) exhibit three-phase equilibrium at low temperatures, while surfactants with extreme solubility preferences yield only two-phase equilibrium. For systems which exhibit three-phase equilibrium, at low temperatures the three-phase region is surrounded on two sides by two-phase envelopes and the surfactant is immiscible with both water and oil over a large composition range. An increase in temperature yields a third two-phase region below the three-phase triangle. As the temperature is increased further, the three-phase region is eliminated, resulting in a stable two-phase region overlapping a smaller metastable envelope. For hydrophilic (hydrophobic) surfactants, the miscibility gap with water (oil) is eliminated first, followed by loss of immiscibility with oil (water) at higher temperatures. Decreasing the number of surfactant contacts available for solvation by imposing rigidity promotes a transition from three- to two-phase equilibrium. Increasing the oil chain length for a system which exhibits

two-phase equilibrium first results in emergence of a three-phase triangle, followed by a reversion to two-phase equilibrium with reversed surfactant solubility.

V. FUTURE WORK

As discussed in Sec. II, the interaction energies employed for this study are expected to capture the basic features of surfactant systems, but contain several simplifications. For example, they do not promote water-head or oil-tail interactions and they neglect electrostatic repulsion between ionic head groups. A more detailed model which allows arbitrary head and tail interactions (i.e., does not require heads to be energetically equivalent to water or tails to be energetically equivalent to oil) and a study of Gemini surfactant phase behavior as a function of energetics are warranted.

The complete phase diagram of a surfactant system generally consists of two distinct regions; phase separation at low surfactant concentrations and microstructure self-assembly at higher surfactant concentrations. As the QC theory is incapable of incorporating long-range order effects, microstructure studies should be performed by canonical ensemble Monte Carlo simulations. Questions of importance in this area are the final equilibrium structures as a function of temperature, composition, surfactant structure, and rigidity.

A comparison of our theoretical results to experimental data are not provided as the phase behavior of Gemini systems has not been studied extensively and insufficient data are available. Experimental studies designed to verify the model predictions should be pursued.

ACKNOWLEDGMENTS

The authors gratefully acknowledge financial support from the Rhone-Poulenc Complex Fluids Laboratory and a National Science Foundation fellowship to K.M.L. After the submission of this manuscript K.M.L. was tragically killed in an accident. This paper is dedicated to the memory of a wonderful student, scholar, and person.

- ¹F. M. Menger and C. A. Littau, *J. Am. Chem. Soc.* **115**, 10083 (1993).
- ²H. Eibl, J. McIntyre, E. Fleer, and S. Fleischer, *Methods Enzymol.* **98**, 623 (1983).
- ³R. Zana, M. Benraou, and R. Rueff, *Langmuir* **7**, 1072 (1991).
- ⁴D. Danino, Y. Talmon, H. Levy, G. Beinert, and R. Zana, *Science* **269**, 1420 (1995).
- ⁵M. Rosen, *CHEMTECH*, **30**, 30 (1993).
- ⁶R. Zana and Y. Talmon, *Nature (London)* **362**, 228 (1993).
- ⁷R. Larson, L. Scriven, and H. Davis, *J. Chem. Phys.* **83**, 2411 (1985).
- ⁸R. Larson, *J. Chem. Phys.* **89**, 1642 (1988).
- ⁹A. Mackie, K. Onur, and A. Panagiotopoulos, *J. Chem. Phys.* **104**, 3718 (1996).
- ¹⁰K. Binder, *Z. Phys. B* **43**, 119 (1981).
- ¹¹K. Kaski, K. Binder, and J. Gunton, *Phys. Rev. B* **29**, 3996 (1984).
- ¹²K. Binder and D. Heermann, *Monte Carlo Simulation in Statistical Physics-An Introduction* (Springer, Berlin, 1988).
- ¹³M. Rovere, D. Heermann, and K. Binder, *J. Phys.: Condens. Matter* **2**, 7009 (1990).
- ¹⁴M. Rosenbluth and A. Rosenbluth, *J. Chem. Phys.* **23**, 356 (1953).
- ¹⁵E. Guggenheim, *Mixtures* (Oxford University Press, New York, 1952).
- ¹⁶H. Tompa, *Polymer Solutions* (Academic, New York, 1956).